RESEARCH PAPER

CrossMark

Mechano-nanofluidics: water transport through CNTs by mechanical actuation

Wei Cao[1,2] · Jin Wang[3,4] · Ming Ma[1,2,3]

Abstract

Mechano-nanofluidics, defined as the study of mechanical actuation effects on the properties of nanofluidics, have received broad interest recently in the field of nanofluidics. The coupling between phonons in carbon nanostructures and fluids under confinement is verified to enhance the diffusion of fluids. Especially, carbon nanotubes (CNTs) are applied as perfect nanochannels with fast water mass transport, making them to be one of the next generation of membranes. Here, we investigated water permeation through CNT membranes with the mechanical vibrations using non-equilibrium molecular dynamics simulations. The simulation results reveal that the water flux is highly promoted by a travelling surface waves at 1 THz. The water flux is enhanced by as large as 20 times for the single-file structured water at 20 MPa. The vibration effect is verified to be equivalent to a pressure drop with ΔP up to 295 MPa. We show that the role of vibration diminishes for water in a larger CNTs. The water structure and hydrogen bond network are analyzed to understand the phenomena. The results of the present work are applied to provide guidance for the development of high-performance membranes.

Keywords Nanofluidics · Water transport · Carbon nanotube · Vibration

1 Introductions

Water transport in carbon nanotubes (CNTs) has received broad interest because of the ultra-fast nanofluids mass transport and promising applications in membrane separations (Werber et al. 2016), energy-related fields (Secchi et al. 2016b), and biological entities (Tunuguntla et al. 2017). In recent decades, a lot of experiments and molecular dynamics (MD) simulations have reported the unexpectedly high-water flow rates in CNTs (Holt et al. 2006; Qin et al. 2011; Thomas and McGaughey 2009). The fast water transport is often attributed to the frictionless interfaces of water-CNTs (Falk et al. 2010; Ma et al. 2011). However, the exact mechanism of water transport in CNTs remains unclear. This is because of a lack of experimental outputs, and the divergence of the existing results (Cao et al. 2018a; Kannam et al. 2017). Recently, Secchi et al. (2016a) overcame the problem of estimating the minuscule amounts of water, and revealed an unexpected large and radius-dependent slippage of water transport through individual CNTs. This work provides the challenges to the understanding of nanofluidics, while the experiments are still in their fancy.

MD simulations play an important role in fluid flow in nanochannels (Kannam et al. 2017). When comes to water in CNTs, the simulation results do not provide a satisfactory insight into the fundamental mechanism, failing to explain the experimental trend (Calabro 2017; Zhu et al. 2016). The models and setups are considered to affect the simulation results very much (Thomas and Corry 2015). A recent MD simulation study has reported the fast water diffusion resulted from the coupling between the phonon modes of the CNTs and the running water, by controlling the flow velocity of water down to centimeters per second, which

✉ Ming Ma
maming16@mail.tsinghua.edu.cn

[1] State Key Laboratory of Tribology, Tsinghua University, Beijing 100084, China

[2] Department of Mechanical Engineering, Tsinghua University, Beijing 100084, China

[3] Center for Nano and Micro Mechanics, Tsinghua University, Beijing 100084, China

[4] Department of Engineering Mechanics, Tsinghua University, Beijing 100084, China

is comparable to experimental velocities (Ma et al. 2015). The phonon modes of the CNTs were verified to be able to transfer momentum to water, leading to a nearly three times increase in water diffusion in CNTs. These developments have led to an emerging field called mechano-nanofluidics, which studies the effects of mechanical actuation on the properties of nanofluidics (Cao et al. 2018b).

The development of mechano-nanofluidics is to explore techniques to actuate a specific phonon mode within the confining materials. We aim to excite the confined fluid in a controlled manner. The study could borrow much from microscale acoustofluidics, which is the microfluids manipulation by the propagation of surface acoustic waves (SAW) (Friend and Yeo 2011). The acoustofluids at nanoscale is different due to the non-Fickian fluid flow in nanochannels (Bocquet and Charlaix 2010). The fabrication of SAW-actuated nanofluidic channels made of a piezoelectric material is difficult compared to that at microscale (Miansari and Friend 2016). For water confined in CNTs, the frictionless tube walls and the peculiar hydrogen bond (h-bond) network should be concerned (Bernardina et al. 2016). The specific phonon vibration has been expected to induce a fast water flow. This is often demonstrated in thermo-osmotic motion of water along CNTs driven by collision frequency of water. The continuous water flow were found by either heating the water reservoir (Fu et al. 2018), or the nanoparticles in the reservoir (Zhao and Wu 2015). Another example known as thermophoresis shows a net water flow by imposing an axial thermal gradient along CNT surfaces (Oyarzua et al. 2018). The longitudinal phonon oscillations with a frequency of about 0.03 THz in CNTs has been verified to be the driving force. This mode is also verified theoretically to enhance nanofluids diffusion through a synchronization mechanism (Wang et al. 2018). Other phonon vibrations of CNTs have been proposed to increase the confined fluids flux by mechanical actuations, such as the radial breathing mode (Zhang et al. 2013), and mechanical wave propagation by bending (Qiu et al. 2011), buckling (Kuang and Shi 2014; Zhou et al. 2015), and twisting (Duan and Wang 2010) carbon atoms in CNTs, and Rayleigh traveling waves (Insepov et al. 2006) along nanotubes. The simulation shows that water flux is dependent on the resonant frequency in the terahertz region and the asymmetry of the system (De and Aluru 2018). Those results focus on the water pump in CNTs through mechanical actuation, but a thorough understanding of the phonon vibration of CNTs in a membrane separation process, e.g. by a pressure gradient, is still worth discussing.

In this work, we report a study on water transport through CNT membranes performed by non-equilibrium MD simulations. To reveal the role of a specific phonon vibration separately, the vibration mode was added to the carbon atoms of CNTs manually. We note that this work intends to explore an optimal vibration mode of CNTs at a certain frequency for

water flux. The vibration models studied here are difficult to be realized with existing technologies. But a properly tuned laser excitation is expected to be applied to trigger phonons in CNTs. This could possibly prepared by picosecond and femtosecond laser ultrasonic which could generate waves in the THz range (Babilotte et al. 2010). Here, we studied the water flow through (6, 6) CNTs with single-file water structures and (8, 8) CNT with layered water structures. The relation between the surface vibration and the confined water structures was investigated to understand the mechanisms.

2 Models and methods

2.1 Simulation models

In this work, we refer to the effect of mechanical actuation of CNTs on the water transport. The travelling surface waves were generated by adding periodic displacement directly to all the carbon atoms of CNTs. The intramolecular force in CNTs was not calculated. We also performed two standing waves with the wave number equals to zero for comparison. The actuation styles studied in this work are described according to the equation of motion as follows:

(1) Radial breathing vibration:

For travelling wave:

$$u(t,z) = Ax/d\cos(2\pi f(t - z/c)),$$
$$v(t,z) = Ay/d\cos(2\pi f(t - z/c)),$$
$$w(t,z) = 0, \ k = 2\pi/d.$$

For standing wave:

$$u(t,z) = Ax/d\cos(2\pi ft), \ v(t,z) = Ay/d\cos(2\pi ft), \ w(t,z) = 0, \ k = 0.$$

(2) Travelling bending vibration:

$$u(t,z) = A\cos(2\pi f(t - z/c)), \ v(t,z) = 0, \ w(t,z) = 0, \ k = 2\pi/d.$$

(3) Longitudinal vibration:

$$u(t,z) = 0, \ v(t,z) = 0, \ w(t,z) = A\cos(\omega t), \ k = 0$$

In these equations, u, v, and w represent the displacement along x, y and z axes, respectively. The z axis is the direction along the tube axis. A is the amplitude, f is the frequency, c is the phase velocity, and k is the wave number, where $k = 2\pi f/c$, with the direction being the same as pressure drop. In the simulations, A was set to be 5% of the tube diameter, d. This percentage is comparable to the one observed in experiments of the breathing mode of CNTs (Liu et al. 2013). The effect of water on phonon vibration of CNTs is neglected. We studied a serial of f to observe the frequency dependence with the value ranges from 10 GHz to 10^5 GHz. The travelling waves of breathing and bending modes, standing breathing and longitudinal modes are

Fig. 1 **a** Four kinds of static structure of mechanical vibrations of CNTs, including travelling breathing mode (TBM), travelling bending mode (TBEM), breathing mode (BM), and longitudinal mode (LM). **b** Geometry of the membrane separation system. The green atoms represent the CNTs. **c** Resultant pressures profiles along the CNT axial direction for various applied forces, generated from (6, 6) CNTs simulations. The inset panel shows the results in the red dashed frame. The dashed black lines indicate the positions of the atoms on the edges of CNTs. (Color figure online)
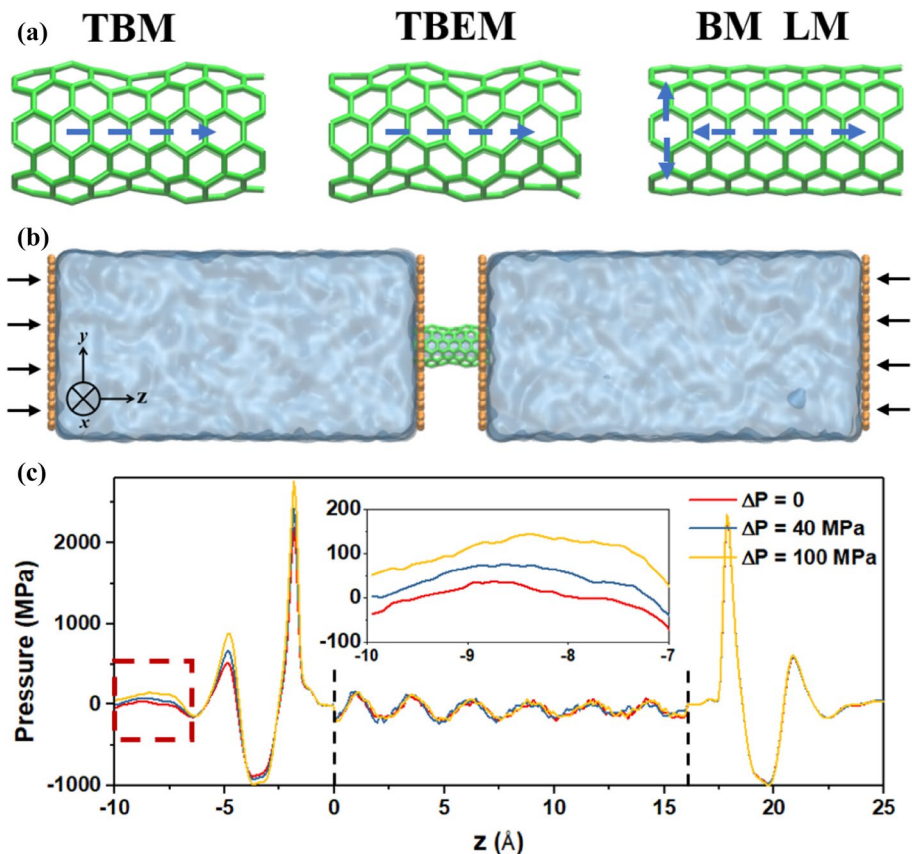
depicted as TBM, TBEM, BM, and LM for short. The static structures of the models can be found in Fig. 1a.

Armchair CNTs were applied to transport water, with the chiral index set to (6, 6) and (8, 8). The diameter d equals to 0.814 and 1.086 nm, respectively. It is anticipated that the solid-like water structures in narrow CNTs could be promoted effectively due to the relatively stable h-bond networks (Striolo 2006). The length of CNTs was chosen to be twice of the diameter, which is 1.6 and 2.2 nm for (6, 6) and (8, 8) CNT, respectively. Water transport through CNTs was performed by non-equilibrium MD simulation methods. Figure 1b presents a schematic picture of the simulation box containing the membrane and two reservoirs. The membrane consists of a CNT and two rigid graphene plates. Each water bath size in the x and y dimensions is 4 nm, and in the z dimension is 8 nm. The system contains 8000 water molecules. Periodic boundary conditions are imposed in all directions. The pressure gradient along the membranes is obtained by the constant force applied on the rigid pistons on both sides. The low pressure was set to 1 bar through adding force to the left piston, therefore only the high pressure was changed. Five pressure drops were considered with ΔP ranges from 0 to 100 MPa. The pressure profile along z direction can be found in Fig. 1c. The pressure gradient varied in the interior and at the entrance/exit points. The

pressure of water inside nanotubes distributes as a wave, showing the spring-like water movement.

2.2 MD methods

All simulations were performed using the LAMMPS software packages. Carbon atoms of CNTs were modeled as unchanged Lennard-Jones (L-J) particles with parameters of $\varepsilon_{c-c} = 0.07$ kcal/mol and $\sigma_{c-c} = 0.355$ nm (MacKerell et al. 1998). Water molecules were modeled with TIP3P force filed (Jorgensen et al. 1983). The cross-term interactions were estimated using the Lorentz–Berthelot mixing rules. The short-range van der Waals were computed with a cutoff distance of 1.0 nm and long-range electrostatic interactions were calculated with the particle–particle–particle–mesh (PPPM) method (Pollock and Glosli 1996).

The simulation system was first minimized with the carbon atoms being froze. The initial velocities were assigned to water according to the Boltzmann distribution. The dynamics of Newton's equation were iterated using a 2.0-fs time step. After minimization, the system was equilibrated at 298 K and fully coupled to a Nose–Hoover thermostat for 2 ns. Those thermostats were applied to all water molecules. The temperature of water near vibrating surfaces would possible be elevated. While this effect is

not considered in this work, to address this problem, we compared our results with the ones that only thermostat water molecules outside CNTs. The difference of water flux among them was found to be neglected. Afterwards, the pressure drop was exerted on the pistons, according to $\Delta P = F_{ave} N_{carbon} / Area_{gra}$, where F_{ave} is the average force exerted on each carbon atoms (the total number is N_{carbon}) of the graphene piston. The mechanical actuations studied in this work were realized by adding specific periodic displacement to the carbon atoms in CNTs according to the equations aforementioned. The interactions between carbon atoms were not considered in the simulations. The simulations run for another 2 ns. After the steady state of water flow across the membrane reached, the time evolution of number of molecules in the reservoirs is recorded for 6 ns.

3 Results and discussion

3.1 Water flux

Figure 2 shows the water flux versus vibration frequency and the transmembrane pressure drop for two CNTs, i.e. (6, 6) and (8, 8). The two CNTs were chosen due to the stable chain-like structures of confined water inside the tubes. Additionally, a CNT with a diameter less than that of (8, 8) CNT is recognized to reject most hydrated ions, which is efficiently applied as desalination membranes (Corry 2017). Note that we do not include ions in the calculations for simplicity. Here, the water flux is obtained by the linear fitting of the number of water molecules passing from the feed to the permeate as a function of simulation time. As discussed before, water in narrow CNTs has been reported to move in waves with a certain eigen frequencies, i.e. 2–14 THz for water in (6, 6) CNTs (Li et al. 2016). Thus, water can adsorb energy from CNTs at this frequency range, showing
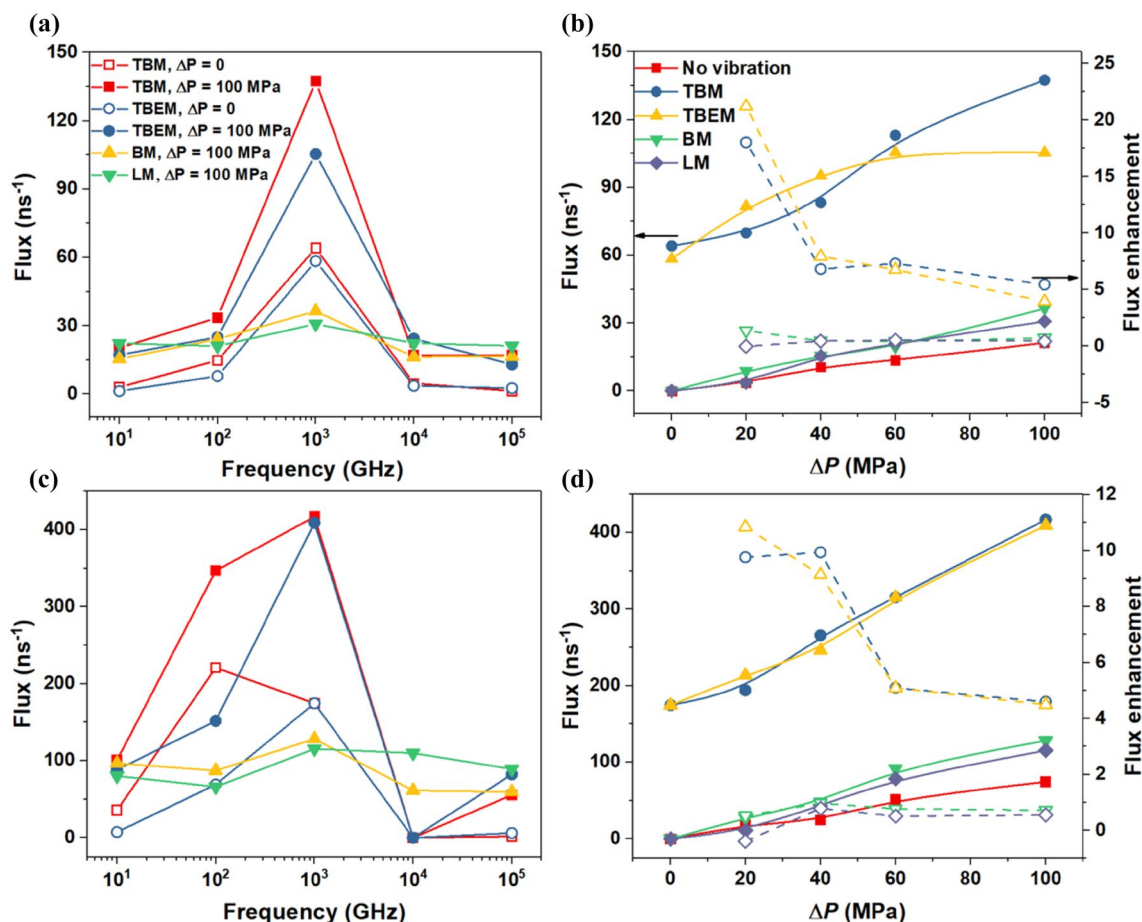

Fig. 2 Flux as a function of vibration frequency (**a, c**) and pressure drop (**b, d**) for water transport through (6, 6) (**a, b**) and (8, 8) (**c, d**) CNTs. The dashed lines in figure **b, d** indicate the flux enhancement, calculated by $\varepsilon = (J_v - J_{no})/J_{no}$ at 1 THz, where J_v, J_{no} is the flux with and without surface vibrations under an identity ΔP, respectively

a resonance between them (Zhang et al. 2013). Figure 2a shows a dependence of water flux on the vibration frequency. Water transport through CNTs is largely enhanced by the actuations, the maximum flux is achieved with the frequency equals to 1 THz for all the four mechanical systems. Here, the characterize frequency as a little smaller than the predicted resonant ones. We attribute this behavior to the phase changes of water resulted from the actuations, due to the open-ended models applied. The phase behavior would be discussed later. Similarly, the optimal frequency is ~ 1 THz for water transport through (8, 8) CNTs (see Fig. 2c). However, the frequency tends to shift to lower values, especially for TBM. In a larger CNTs, water molecules could move more freely and the h-bonds are more likely to break. The range of vibration frequency accessed by water in (6, 6) CNTs is estimated to be much wider and larger than that in (8, 8) CNTs (Thomas et al. 2010). We also note that no water flow in (8, 8) CNTs at 10 THz with the travelling waves, which is not found in (6, 6) CNTs. The vibrating accessible spaces along the axial direction in tube entrances at 10 THz hinder the water passages.

Generally, the travelling waves are applied to overcome the large surface and viscous force in nanofluidics. For water confined in CNTs, the shear in a single file or a layered structured water is rather difficult. The hydrophobic nature of carbon is also not favorable in these processes compared to hydrophilic surfaces (Xie and Cao 2017). Despite these disadvantages, fast water flux is found as a result of resonance. This is attributed to the springs-like water structures in narrow CNTs. The large hydrodynamic slip would also facilitate the water transport driven by surface waves (Fu et al. 2017). The driving force is different among the four types of vibrations studied in this work. The TBM is analogous to Rayleigh wave, through which water molecules move with the wave by the multiple reflections from the tube wall. It has been reported that the friction force is the driving force for gases flow in CNTs by TBM, with the velocity at the order of km/s (Insepov et al. 2006). The velocity is larger than that of water calculated in this work. Nevertheless, the frequency needed to drive the gas is found to be much higher than that for water. For TBEM, the water driving force is recognized to be the centrifugal force (Qiu et al. 2011). Water molecules are forced to vibrate with the tubes and move along the direction of wave propagation. For standing waves, i.e. BM and LM, water flux is obtained by the resonance between water and CNTs. The water transport is not comparable to that by travelling waves. The largest water flux in (6, 6) CNTs is found to be about twice the value without vibrations, which is consistent with the literature (Zhang et al. 2013). LM actuation is verified theoretically to enhance water flux through a synchronization mechanism as aforementioned. The water fluxes are a little less than those actuated by BM.

The relation between the water flux and pressure drop is depicted in Fig. 2b for (6, 6) CNT and 2d for (8, 8) CNT. Water transport through CNTs without an actuation is found to obey Darcy's law (Zarandi et al. 2018), which is represented as $J \propto \Delta P$. Inversely, in Fig. 2b, the water flux does not increase monotonically with pressure drop, especially for travelling wave systems. The nonlinear relationship is the result of the change of resistance with pressure. The transfer process can be described according to $J = (\Delta P + F/A)/R$, where J is water flux, F/A is the force driven by vibrations, R is the resistance, $R = R_{en} + R_{in}$, R_{en} is the resistance in the entrance/exit region and R_{in} is the resistance inside CNTs. R_{en} is calculated by $3\eta/8d^3$, where η is the shear viscosity of water. The inertial losses at the two CNT-reservoir boundaries has been also reported to be a factor (Thomas and McGaughey 2009). For water flow through CNTs, R_{in} can be often neglected because of the frictionless of CNTs. Therefore, we can estimate R_{en} by the slope of the $J - \Delta P$ line of water in CNTs with no vibrations. From the figure, we thus can find that R_{en} decreases for water in CNTs as an effect of waves, indicating that water molecules have a larger opportunity to enter the vibrating tubes. We refer to the resistance change to the change of the water density and h-bonding stability (see Figs. 3, 4). The rough surfaces resulting from travelling waves would also amplify the shear force between water and CNTs and R_{in}. For TBEM and TBM in (6, 6) CNTs, we find that the resistance, R, increases with the pressure from the curve in Fig. 2b. While for TBM, R would decrease with increasing pressure. For water transport through (8, 8) CNTs, the nonlinear relationship is not so obvious.

The effect of vibration is further addressed by analyzing the flux enhancement, calculated by $\varepsilon = (J_v - J_{no})/J_{no}$ under each ΔP, where J_v, J_{no} is the flux with and without surface vibrations at an identity ΔP, respectively. In Fig. 2b, d, we present the variation of ε with ΔP shown as dashed lines. Here, we find that ε decreased monotonically with increasing ΔP. That is, the vibration is more efficient under a smaller pressure difference across CNT membranes. In the calculations of (6, 6) CNTs, the largest enhancement is 21.2 for TBEM at 20 MPa, 1 THz. From the figure, we also find that the enhancement as an effect of travelling waves is much larger than that with standing waves. For instance, ε equals to 1.4 for BM, compared to 18 for TBM with the wave propagation. Additionally, the enhancements of two travelling waves and two standing waves are found to be comparable, respectively. For water transport through (8, 8) CNTs, the role of mechanical actuation is weakened compared to that of (6, 6) CNT. The result can be understood by the faster self-diffusion of water in (8, 8) CNTs, compared to the collective movement of single-file water in (6, 6) CNTs. The thermo motion of water in (8, 8) CNTs would hinder the resonant motion actuated by surface vibrations.
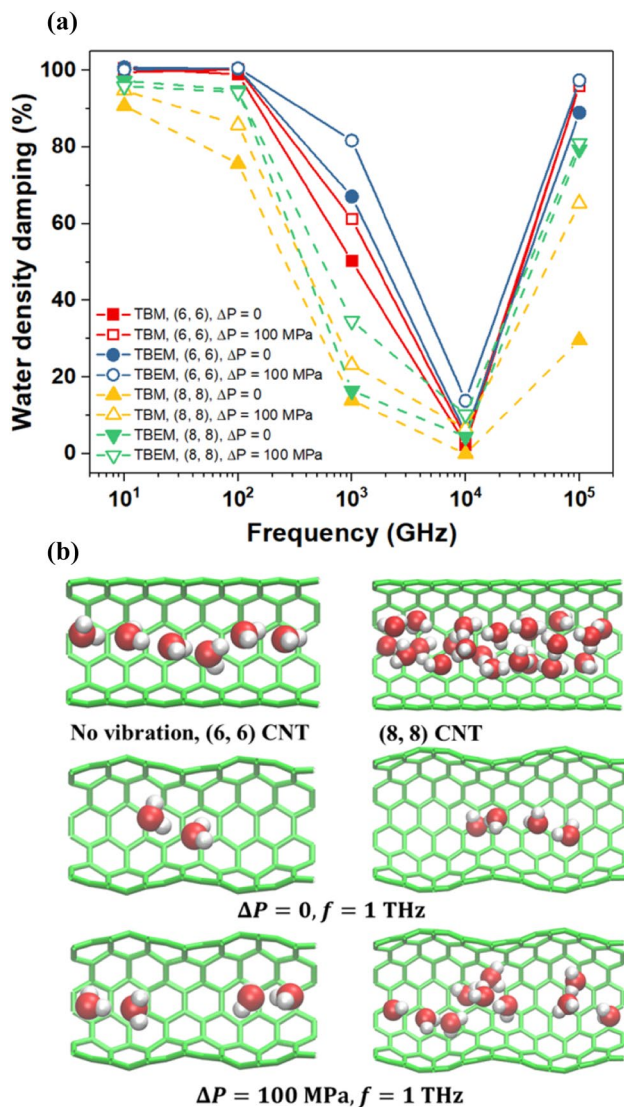
(a)

(b)

Fig. 3 Density damping (**a**), ρ_v/ρ_{no}, versus vibration frequency. The solid and dashed lines are for (6, 6) and (8, 8) CNT, respectively. **b** Representative water structures as a result of pressure drop and vibration frequency. The results of TBM are shown

The largest enhancement of water flux through (8, 8) CNTs is 10.8, for TBEM at $\Delta P = 20$ MPa, $f = 1$ THz. Finally, we emphasize the water flux under travelling waves without a pressure drop, indicative of the actuation effect of water transport. The largest water flux in (6, 6) CNTs is found to be 64.1 ns^{-1} and 58.4 ns^{-1} for TBM and TBEM at 1 THz, respectively. This vibration effect is equivalent to a pressure drop with ΔP equals to 295 MPa and 269 MPa. These values are estimated by first linear fitting the water flux with pressure drop under no actuation, and then extrapolating to the specific flux to get a pressure drop. For water transport through a larger (8, 8) CNT, the flux for TBM and TBEM at 1 THz is both calculated to be 174.6 ns^{-1}, corresponding to a ΔP of 230.5 MPa.

3.2 Water molecular dynamics

In an effort to elucidate the highly water flux increments through travelling surface waves studied in this work, we first analyzed the water depletion in CNTs. We plot in Fig. 3 the water density damping versus frequency, calculated by ρ_v/ρ_{no}. It is clear that as the frequency increases, significant less water molecules occupy the nanotubes. Water content in CNTs further increases with the frequency up to 100 THz. At this frequency, the confined water molecules hardly feel the vibrations. The depletion of water under surface waves is predictable due to the energy transfer from the surface to water. The water evaporation on surfaces under such wave propagation is applied to drive fluids through microchannels (Cecchini et al. 2008). Previously, the entropy dominated vapor-like phase for water in (6, 6) CNTs and enthalpy dominated ice-like phase for water in (8, 8) CNTs have been reported (Pascal et al. 2011). For TBM and TBEM here, the enthalpic penalty is expected to be amplified. This simple picture of unfavorable enthalpy due to the decreasing average number of h-bonds per water molecules in CNTs, represented as $\langle n_{HB} \rangle$, as seen from Fig. 4. Similarly, the entropy gain of water should also arise from the increase of the rotation degree of freedom. The rotation entropy change should come from the travelling waves and the heterogeneous phase space sampling along the tube axis. Therefore, it is anticipated from thermodynamics that water would have a larger possibility to enter the vibrating CNTs. However, the relative continuum water flow through nanotubes breaks up with water depletion. This phenomenon weakens the momentum transfer from reservoir to water inside CNTs, further diminishes the role of pressure difference on the water passage.

It is observed that the density damping reaches the maximum at $f = 10$ THz. Water molecules are found to be hard to transport through CNTs at this frequency, especially for (8, 8) CNT. We image that once the water molecules enter the tube and then are "squeezed out" by the surface wave at a short time. Moreover, we find that the difference of the water density damping between different pressure at 1 THz is larger than other frequency. The result supports the finding of the nonlinear change of water flux with pressure (see Fig. 2). The vibration effect on water density also varies between different CNTs. Despite the smaller enhancement of water flux actuated by surface waves, the larger water density decrease is found for water in (8, 8) CNTs, compared to that for (6, 6) CNTs. In (8, 8) CNTs, the depletion of water means water can diffuse more freely to the center of tube, indicative of the less impact by surface wave. To better elucidate the phase change, we provide the representative water structures as a result of pressure drop and vibration frequency for TBM, as shown in Fig. 3b. The vibration of CNTs induces a dominant phase change, i.e. from the current
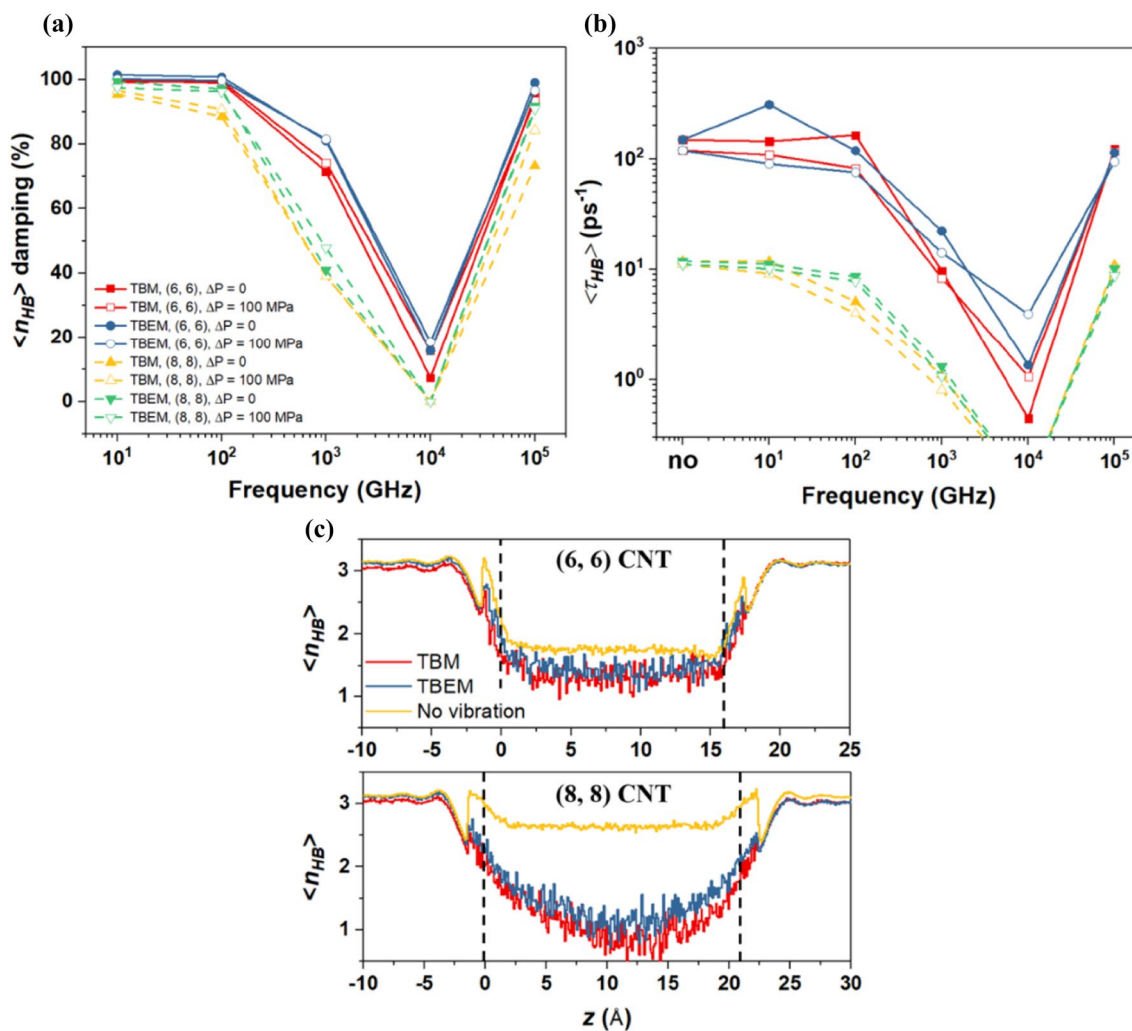
Fig. 4 The average hydrogen bond damping (**a**), $\langle n_{HB} \rangle_v / \langle n_{HB} \rangle_{no}$, and average hydrogen bond relaxation time (**b**), τ_{HB}, versus vibration frequency. The solid and dashed lines are for (6, 6) and (8, 8) CNT, respectively. **c** The $\langle n_{HB} \rangle$ distribution along the CNT axial direction for various vibration modes at 1 THz, 100 MPa

state to a non-wetting state under no pressure. The non-wetting state would transit to a liquid-like state when the pressure increases to 100 MPa. We anticipate the density would further increase with increasing pressure. The phase transition behavior is similar to that expected for different temperatures (Agrawal et al. 2017).

The dynamic of water is revealed by the h-bond network of confined water. The h-bond network is characterized by both the average h-bond number, n_{HB}, and the average relaxation time, τ_{HB}. The relaxation time is calculated by $\tau_{HB} = \int_0^\infty t p_{HB}(t) dt$, where $p_{HB}(t)$ is the probability density of h-bond breaking. Figure 4 shows the h-bond damping, calculated by $\langle n_{HB} \rangle_v / \langle n_{HB} \rangle_{no}$, and $\langle \tau_{HB} \rangle$ of water as a function of frequency. The changes of both the $\langle n_{HB} \rangle$ and $\langle \tau_{HB} \rangle$ with frequency are accordant with those of water density. The $\langle \tau_{HB} \rangle$ variation is also supportive to the phase change stated previously. The stability of the chain-like water

structures is verified by $\langle \tau_{HB} \rangle$. We compare these values with the residence time, τ_{res}, and find that they are smaller. The results suggest that the h-bond network is undergoing continuous breaking and re-forming. Especially, the $\langle \tau_{HB} \rangle$ decreases with the increasing pressure. The trend reminds us the aforementioned large enhancement factor under a small pressure drop. The water molecules under a large pressure would be more unstable. The frequent h-bond breaking and re-forming would lead to an energy penalty, and further reduce the water flow through CNTs. Additionally, the $\langle n_{HB} \rangle$ distribution along the CNT axial direction for various vibration modes at 1 THz and 100 MPa is plotted in Fig. 4c. The $\langle n_{HB} \rangle$ drops rapidly at the entrance to the membrane, indicating that there is an energetic penalty incurred as a molecule enters the membrane. We also find the large fluctuation inside tubes with a surface wave compared to that with no vibration. This shows the non-continuum water flow in
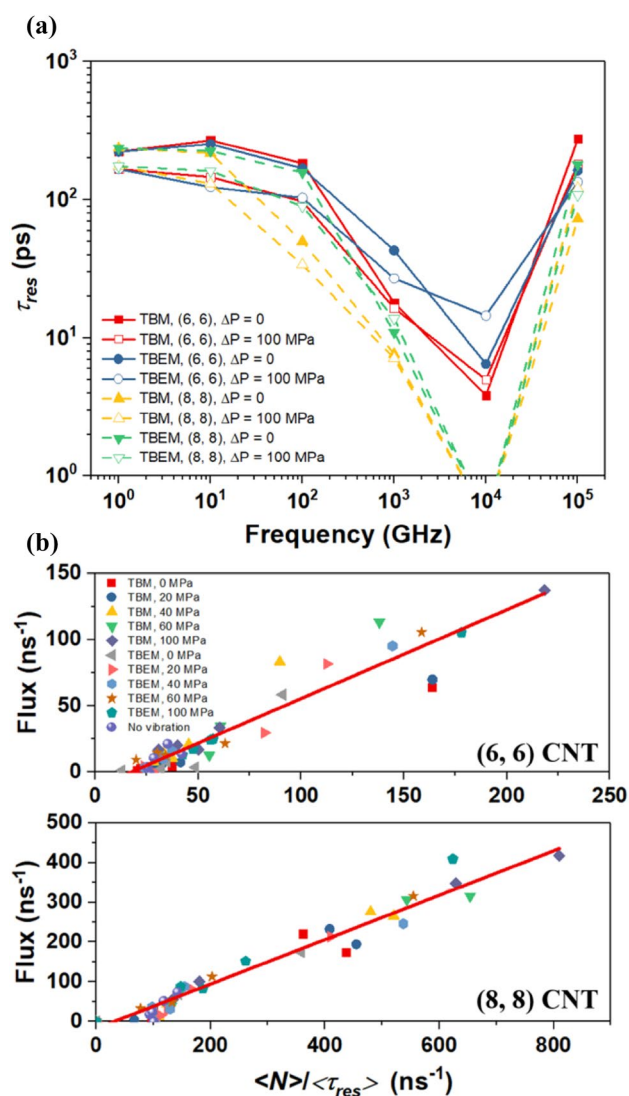
(a)

(b)

Fig. 5 **a** The relaxation time, τ_{res}, versus vibration frequency. **b** Water flux versus average number of water molecules inside CNTs, $\langle N \rangle$, divided by average residence time. The symbols are the simulation data for TBM and TBEM. The solid lines are the linear fit to these data

CNTs. The fluctuation is more obvious for water in a larger CNTs, which is consistent with the larger water depletion.

The residence time is calculated by $\tau_{res} = \int_0^\infty t p_{res}(t) dt$, where $p_{res}(t)$ is the probability density of leaving CNTs. The residence time distribution reveals information regarding the degree of mixing of water molecules in the CNTs. From Fig. 5a, the curves have the similar patterns with Fig. 4b. Although the residence time is small at 10 THz, water flux is limited due to that molecules would leave the tube once entering it. Such the relation of τ_{res} suggests that we cannot solely determine the water flux by residence time. An obvious parameter to consider is the number of water molecules occupying the CNTs. It is anticipated

that a combination of the two is able to explain the water flux. We finally fit the water flux with the $\langle N \rangle$ divided by the residence time τ_{res}, as shown in Fig. 5b. Interestingly, a linear relationship exists regardless of the travelling wave styles, pressure drop or frequency. The water flux is expected to be further enhanced by either increase the water occupation or decrease the residence time. The slop for (6, 6) and (8, 8) CNT is estimated to be 0.67 and 0.56. The slightly smaller value in a larger CNT is a result of water diffusion along the radial direction. This linear relation is not found for standing waves, such as BM and LM. We note that the energy dissipation of CNTs resulted from the water molecules inside is not addressed in this work. Therefore, the fitting lines provides upper bounds to the flux enhancement by mechanical actuation.

4 Conclusion

In this study, we have observed the transport of water through CNT membranes actuated by surface vibrations via non-equilibrium molecular dynamics simulations. In particular, we investigated the travelling surface waves including the breathing and bending modes with various frequency, as well as the standing breathing mode and longitudinal mode. The single-file structured water in (6, 6) CNT and circular water structures in (8, 8) are both addressed here. The simulation results reveal that the water flux is highly promoted by a travelling surface wave at 1 THz. The water flux is enhanced by as large as 20 times for the single-file structured water at 20 MPa. The vibration effect is verified to be equivalent to a pressure drop with ΔP up to 295 MPa. We show that the role of vibration diminishes for water in a larger CNTs, due to the relative unstable hydrogen bond network. The water structure and hydrogen bond network are analyzed to understand the phenomena. The phase of water would transit to a non-wetting state with increasing frequency, and then transfer to a liquid-like state with increasing pressure. The result that the hydrogen bond relaxation time declines with pressure also explains the large enhancement under a small pressure drop. Additionally, we find that the water flux is proportional to the water occupation divided by the residence time in CNTs, independent of travelling wave styles, pressure drop and vibration frequency. The above conclusions provide upper bounds to the flux enhancement by mechanical actuation. We believe that the water flux could be further enhanced, i.e. by eliminating the unstable factor in the single-file water chain such as hydrogen bonding defects (Kofinger et al. 2011).

Compliance with ethical standards

Conflict of interest The authors declare no commercial or associative interest that represents a conflict of interest in connection with the work submitted.

Ethical standards Our research does not include human participants and animals. All authors consent the submit to this journal.

References

Agrawal KV, Shimizu S, Drahushuk LW, Kilcoyne D, Strano MS (2017) Observation of extreme phase transition temperatures of water confined inside isolated carbon nanotubes. Nature nanotechnology 12:267–273. https://doi.org/10.1038/nnano.2016.254

Babilotte P et al (2010) Femtosecond laser generation and detection of high-frequency acoustic phonons in GaAs semiconductors Physical Review B 81 https://doi.org/10.1103/PhysRevB.81.245207

Bernardina SD, Paineau E, Brubach J-B, Judeinstein P, Rouziere S, Launois P, Roy P (2016) Water in Carbon Nanotubes: The Peculiar Hydrogen Bond Network Revealed by Infrared Spectroscopy. J Am Chem Soc 138:10437–10443. https://doi.org/10.1021/jacs.6b02635

Bocquet L, Charlaix E (2010) Nanofluidics, from bulk to interfaces. Chem Soc Rev 39:1073–1095. https://doi.org/10.1039/b909366b

Calabro F (2017) Modeling the effects of material chemistry on water flow enhancement in nanotube membranes. Mrs Bulletin 42:289–293. https://doi.org/10.1557/mrs.2017.58

Cao W, Huang L, Ma M, Lu L, Lu X (2018a) Water in Narrow Carbon Nanotubes: Roughness Promoted Diffusion Transition The. J Phys Chem C 122:19124–19132. https://doi.org/10.1021/acs.jpcc.8b02929

Cao W, Wang J, Ma M (2018b) Carbon nanostructure based mechano-nanofluidics. J Micromech Microeng 28:033001

Cecchini M, Girardo S, Pisignano D, Cingolani R, Beltram F (2008) Acoustic-counterflow microfluidics by surface acoustic waves. Appl Phys Lett 92:104103. https://doi.org/10.1063/1.2889951

Corry B (2017) Mechanisms of selective ion transport and salt rejection in carbon nanostructures. Mrs Bulletin 42:306–310. https://doi.org/10.1557/mrs.2017.56

De S, Aluru NR (2018) Energy Dissipation in Fluid Coupled Nanoresonators: The Effect of Phonon-Fluid Coupling. ACS Nano 12:368–377. https://doi.org/10.1021/acsnano.7b06469

Duan WH, Wang Q (2010) Water Transport with a Carbon Nanotube. Pump Acs Nano 4:2338–2344. https://doi.org/10.1021/nn1001694

Falk K, Sedlmeier F, Joly L, Netz RR, Bocquet L (2010) Molecular Origin of Fast Water Transport in Carbon Nanotube Membranes: Superlubricity versus Curvature Dependent. Friction Nano letters 10:4067–4073. https://doi.org/10.1021/nl1021046

Friend J, Yeo LY (2011) Microscale acoustofluidics: Microfluidics driven via acoustics and ultrasonics. Rev Mod Phys 83:647–704. https://doi.org/10.1103/RevModPhys.83.647

Fu L, Merabia S, Joly L (2017) What Controls Thermo-osmosis? Molecular Simulations Show the Critical Role of Interfacial Hydrodynamics. Phys Rev Lett 119:214501. https://doi.org/10.1103/PhysRevLett.119.214501

Fu L, Merabia S, Joly L (2018) Understanding Fast and Robust Thermo-Osmotic Flows through Carbon Nanotube Membranes. Thermodynamics Meets Hydrodynamics The journal of physical chemistry letters. https://doi.org/10.1021/acs.jpclett.8b00703

Holt JK et al (2006) Fast mass transport through sub-2-nanometer. carbon nanotubes Science 312:1034–1037. https://doi.org/10.1126/science.1126298

Insepov Z, Wolf D, Hassanein A (2006) Nanopumping Using Carbon Nanotubes Nano letters 6:1893–1895. https://doi.org/10.1021/nl060932m

Jorgensen WL, Chandrasekhar J, Madura JD, Impey RW, Klein ML (1983) Comparison of simple potential functions for simulating liquid water. The Journal of chemical physics 79:926–935. https://doi.org/10.1063/1.445869

Kannam SK, Daivis PJ, Todd BD (2017) Modeling slip and flow enhancement of water in carbon nanotubes. MRS Bull 42:283–288. https://doi.org/10.1557/mrs.2017.61

Kofinger J, Hummer G, Dellago C (2011) Single-file water in nanopores. Physical chemistry chemical physics: PCCP 13:15403–15417. https://doi.org/10.1039/c1cp21086f

Kuang YD, Shi SQ (2014) Strong mechanical coupling between the carbon nanotube and the inner streaming water flow. Microfluid Nanofluid 17:1053–1060. https://doi.org/10.1007/s10404-014-1391-1

Li JY, Wu ZQ, Xu JJ, Chen HY, Xia XH (2016) Water transport within carbon nanotubes on a wave. Physical chemistry chemical physics: PCCP 18:33204–33210. https://doi.org/10.1039/c6cp05773j

Liu K et al (2013) Quantum-coupled radial-breathing oscillations in double-walled carbon nanotubes. Nature Communications 4:1375. https://doi.org/10.1038/ncomms2367

Ma MD, Shen L, Sheridan J, Liu JZ, Chen C, Zheng Q (2011) Friction of water slipping in carbon nanotubes Phys Rev E 83 https://doi.org/10.1103/PhysRevE.83.036316

Ma M et al (2015) Water transport inside carbon nanotubes mediated by phonon-induced oscillating friction. Nature nanotechnology 10:692–695. https://doi.org/10.1038/nnano.2015.134

MacKerell AD et al (1998) All-Atom Empirical Potential for Molecular Modeling and Dynamics Studies of Proteins The. Journal of Physical Chemistry B 102:3586–3616. https://doi.org/10.1021/jp973084f

Miansari M, Friend JR (2016) Acoustic Nanofluidics via Room-Temperature Lithium Niobate Bonding: A Platform for Actuation and Manipulation of Nanoconfined Fluids and Particles. Adv Func Mater 26:7861–7872. https://doi.org/10.1002/adfm.201602425

Oyarzua E, Walther JH, Zambrano HA (2018) Water thermophoresis in carbon nanotubes: the interplay between thermophoretic and friction forces Physical chemistry chemical physics. PCCP 20:3672–3677. https://doi.org/10.1039/c7cp05749k

Pascal TA, Goddard WA, Jung Y (2011) Entropy and the driving force for the filling of carbon nanotubes with water. Proc Natl Acad Sci USA 108:11794–11798. https://doi.org/10.1073/pnas.1108073108

Pollock EL, Glosli J (1996) Comments on P3M, FMM, and the Ewald method for large periodic Coulombic systems. Comput Phys Commun 95:93–110. https://doi.org/10.1016/0010-4655(96)00043-4

Qin X, Yuan Q, Zhao Y, Xie S, Liu Z (2011) Measurement of the rate of water translocation through carbon nanotubes. Nano letters 11:2173–2177. https://doi.org/10.1021/nl200843g

Qiu H, Shen R, Guo W (2011) Vibrating carbon nanotubes as water pumps. Nano Research 4:284–289. https://doi.org/10.1007/s12274-010-0080-y

Secchi E, Marbach S, Nigues A, Stein D, Siria A, Bocquet L (2016a) Massive radius-dependent flow slippage in. carbon nanotubes Nature 537:210–213. https://doi.org/10.1038/nature19315

Secchi E, Nigues A, Jubin L, Siria A, Bocquet L (2016b) Scaling Behavior for Ionic Transport and its Fluctuations in Individual Carbon Nanotubes Physical Review Letters 116 https://doi.org/10.1103/PhysRevLett.116.154501

Striolo A (2006) The mechanism of water diffusion in narrow carbon nanotubes. Nano letters 6:633–639. https://doi.org/10.1021/nl052254u

Thomas M, Corry B (2015) Thermostat choice significantly influences water flow rates in molecular dynamics studies of carbon nanotubes. Microfluid Nanofluid 18:41–47. https://doi.org/10.1007/s10404-014-1406-y

Thomas JA, McGaughey AJH (2009) Water Flow in Carbon Nanotubes: Transition to Subcontinuum Transport Phys Rev Lett 102 https://doi.org/10.1103/PhysRevLett.102.184502

Thomas JA, Iutzi RM, McGaughey AJH (2010) Thermal conductivity and phonon transport in empty and water-filled carbon nanotubes Physical Review B 81 https://doi.org/10.1103/PhysRevB.81.045413

Tunuguntla RH, Henley RY, Yao Y-C, Tuan Anh P, Wanunu M, Noy A (2017) Enhanced water permeability and tunable ion selectivity in subnanometer carbon. nanotube porins Science 357:792–796. https://doi.org/10.1126/science.aan2438

Wang J, Cao W, Ma M, Zheng Q (2018) Enhanced diffusion on oscillating surfaces through synchronization. Phys Rev E 97:022141. https://doi.org/10.1103/PhysRevE.97.022141

Werber JR, Osuji CO, Elimelech M (2016) Materials for next-generation desalination and water purification membranes. Nature Reviews Materials 1:16018

Xie J-F, Cao B-Y (2017) Fast nanofluidics by travelling surface waves Microfluidics and Nanofluidics 21 https://doi.org/10.1007/s10404-017-1946-z

Zarandi MAF, Pillai M, Kimmel KA (2018) Spontaneous imbibition of liquids in glass-fiber wicks. Part I: usefulness of a sharp-front approach. AIChE J 64:294–305. https://doi.org/10.1002/aic.15965

Zhang QL, Jiang WZ, Liu J, Miao RD, Sheng N (2013) Water Transport through Carbon Nanotubes with the Radial Breathing Mode Physical Review Letters 110

Zhao K, Wu H (2015) Fast water thermo-pumping flow across nanotube membranes for desalination. Nano Lett 15:3664–3668. https://doi.org/10.1021/nl504236g

Zhou X, Wu F, Liu Y, Kou J, Lu H, Lu H (2015) Current inversions induced by resonant coupling to surface waves in a nanosized water pump. Phys Rev E 92:053017. https://doi.org/10.1103/PhysRevE.92.053017

Zhu Y, Lu X, XIE W, Cao W, Lu L, Dong Y, Wu J (2016) The progress of quantitatively description of membrane process based on the mechanism of nanoconfined mass transfer. Chin Sci Bull 62:223–232